Study of micropipe structure in SiC by x-ray phase contrast imaging

V. G. Kohn
Russian Research Center, "Kurchatov Institute", 123182 Moscow, Russia

T. S. Argunova
Ioffe Physico-Technical Institute, RAS, Polytekhnicheskaya St. 26, 194021 St. Petersburg, Russia and X-ray Imaging Center, Department of Materials Science and Engineering, Pohang University of Science and Technology, San 31 Hyoja-dong, Namku, Pohang 790-784, Republic of Korea

Jung Ho Je[a)]
X-ray Imaging Center, Department of Materials Science and Engineering, Pohang University of Science and Technology, San 31 Hyoja-dong, Namku, Pohang 790-784, Republic of Korea

(Received 10 July 2007; accepted 2 October 2007; published online 22 October 2007)

Phase contrast images of dislocation micropipe in SiC crystal are experimentally studied at various distances from the sample using synchrotron white beam. Computer simulation of these images enabled us to understand the peculiarities of image formation and measure the diameter of the micropipe. The phase contrast imaging of micropipes without monochromator is explained by the absorption of x rays in a thick (490 μm) SiC crystal, effectively forming a high brilliance radiation spectrum with a pronounced maximum at 16 keV. © *2007 American Institute of Physics*.
[DOI: 10.1063/1.2801355]

The third generation synchrotron radiation sources provide a powerful tool for imaging microstructures by means of coherent scattering, namely, phase contrast imaging[1] also known as phase sensitive radiography.[2] The source of small angular sizes directly creates a beam of high spatial coherence, but temporal coherence has to be prepared by users. As a rule, high resolution crystal monochromator is used as a multi-purpose device. Recently, the imaging is also realized with a low-resolution monochromator[3,4] or without a monochromator at all,[2] i.e., in a "white beam."

In this work, we applied the white beam phase contrast imaging technique to examine the structure of micropipe in silicon carbide which is an advanced semiconductor material. The micropipe is a crystal grown-in defect, namely, screw superdislocation with a hollow quasicylindrical core[5,6] whose dislocation line is parallel to the pipe axis and whose Burgers vector is connected with the pipe radius.[7] Because micropipes severely affect the SiC device performance, nondestructive methods of characterizing the structure of micropipes are quite useful for both crystal growers and crystal users. Until now, micropipes have been investigated by x-ray topography, optical microscopy, and scanning electron microscopy.[6,8] The white beam phase sensitive radiography for imaging micropipes in SiC that has been recently used[2,9] made it possible to determine the location, the orientation, and the shape of micropipes. However, no quantitative information has been extracted from the images so far. In particular, the estimation of micropipe size is important because the Burgers vector can then be evaluated using the Frank relation,[7] and the nature, the origination, and the transformation of micropipes can be consequently interpreted. The purpose of this work is to apply, in addition to the experimental study, computer simulations of micropipe images to obtain the micropipe diameter.

The phase contrast imaging experimental setup involves a synchrotron radiation source at a large distance from the sample, and a detector placed at different distances behind the sample. Our experiments were performed at the 7B2 X-ray Microscopy Beamline of the Pohang Light Source, Korea. The beam from a bending magnet was created by a source with effective sizes of 160 (H) and 60 (V) μm, located at a distance of 34 m from the sample. X-ray photons were converted into visible light by the 150 μm thick $CdWO_4$ scintillator and were recorded with a charge coupled device camera (14 bit gray scale and 1600×1200 pixels range). The captured image was magnified by a lens system, with magnification from $1\times$ to $50\times$. On the beam path, no objects except beryllium windows were placed.

Typical images of the SiC micropipes are shown in Fig. 1(a). These images are affected strongly by many factors such as beam parameters, the pipe diameter, the angle between the pipe axis and the beam direction, and even by the sample thickness. Usually, the micropipes have been supposed to propagate parallel to the growth axis. However, the

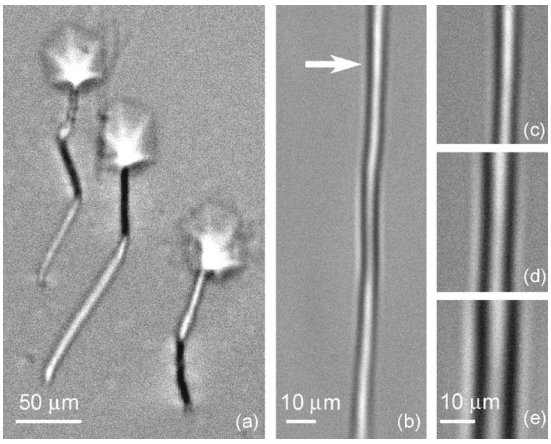

FIG. 1. Typical images of micropipes in SiC wafers cut perpendicular to the [0001] growth direction (a) and along the growth direction (b). The arrow in (b) indicates the fragment shown in (c)–(e) at various sample-to-detector distances: 10, 30, and 50 cm, respectively. Halos in (a) correspond to etch pits on the wafer surface.

[a)]Electronic mail: jhje@postech.ac.kr

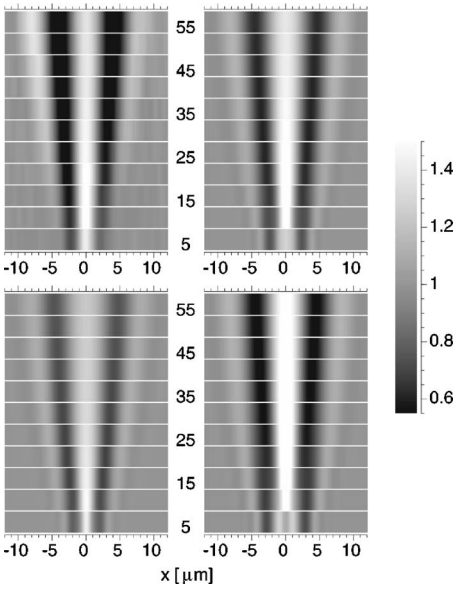

FIG. 2. Distance dependence of the pipe images. The distance values in cm are shown between the panels. The left-top panel shows fragments of the experimental images. The right-top panel shows the simulated images for the pipe of 4 μm diameter. The bottom panels show simulated images for 3 μm (left) and 5 μm (right). The right scale shows the contrast value.

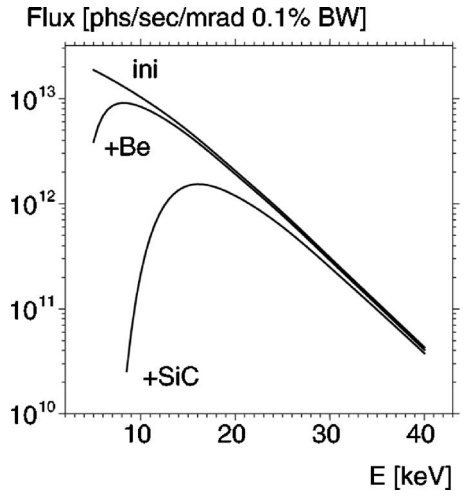

FIG. 3. Synchrotron radiation spectra estimated with and without the absorbers of 2 mm thick Be and 490 μm thick SiC.

images show that the orientation of the pipes is more complicated, and they can remarkably deviate from their initial propagation direction. The images may be white, black, or gray inside. It is not easy to obtain the pipe diameter and the axis orientation directly from the images. Therefore, computer simulations of the images are quite necessary for understanding how the images are formed and for extracting the parameters of pipes by means of comparing the real and simulated images.

To make this work easier, we prepared a special sample, which is axial-cut slice along the growth direction [0001] obtained from 4*H*-SiC boule. The boule was grown in Ar by the sublimation sandwich method[10] at the growth temperature of 2100 °C and with the growth rate of 0.5 mm h^{-1}. The 490 μm thick sample which was mechanically polished on both sides contained micropipes (0.5 to 10 μm in diameter) placed almost parallel to the surface. The sample was rotated to have a horizontal position of the pipe axis, so the edge enhancement of micropipes was obtained in a more coherent vertical direction. Also the surface of the SiC wafer was adjusted so that it would be perpendicular to the beam. We obtained eleven images for the distances from 5 to 55 cm, starting with the first image registered at 5 cm from the sample and increased the distance every 5 cm. As shown in several typical images in Figs. 1(c) and 1(e), the images are sensitive to the distance just because of their coherent nature. The intensity profiles for all 11 distances are shown in the left-top panel of Fig. 2 as 11 stripes of gray computer map.

The computer simulation of synchrotron white beam micropipe images is more complicated than that of monochromatized beam simulation. In reality, coherent scattering occurs only in monochromatic wave. Therefore, the intensity distributions for various monochromatic components of radiation have to be summed up over the real radiation spectrum. This spectrum should be calculated considering all absorbers on the beam path from the source to the detector including the sample itself. We used the spectrum calculated for the beamline and shown in Fig. 3. The initial spectrum (the top curve) was calculated from the data available at the website.[11] The detector placed after the 2 mm thick Be window registers a spectrum shown as the middle curve. The bottom curve demonstrates the spectrum estimated by considering the additional absorption by the 490 μm thick SiC wafer. The spectrum curve shows a pronounced maximum at the energy of 16 keV. Although the decreasing intensity at larger energies is a property of synchrotron radiation, the intensity decrease at smaller energies is attributed to the absorption by the sample. Therefore, the white beam imaging becomes possible because the beam is not completely white but has some finite energy region of higher brilliance.

The source size should be calculated on the intensity level as well, because various points of the source are incoherent. The propagation of the transverse (i.e., x,y) spatial dependence of the coherent wave in free space along the optical axis (i.e., z axis) is described by the convolution with the Kirchhoff propagator $P_K(x,y,z)=P(x,z)P(y,z), P(x,z)=(i\lambda z)^{-1/2}\exp(i\pi x^2/\lambda z)$, where λ is a wavelength of x rays. The coherent wave from the point source is described by the propagator itself. The longitudinal size of the micro-objects is too small to incline the x rays notably. Therefore, the object is characterized by the local transmission function which describes the transverse dependence of the x-ray wave. It is then sufficient to take into account the phase shift and attenuation by the object. For the hollow cylindrical pore of the radius R, the transmission function $T(x)$ would be as follows: $T(x)=\exp[(iP+M)(1-x^2/R^2)^{1/2}]$, where $P=4\pi\delta R/(\lambda \sin\alpha)$, $M=P\beta/\delta$. Here, the parameters δ and β determine the dielectic function ϵ of the sample material so that $\epsilon=1-2\delta+i2\beta$. The angle α between the pipe axis and the z axis was 90° in our calculation. The pore increases both the phase and the amplitude of the x-ray wave, but the main effect is the phase increase because P is several orders larger than M.

Since the transmission function does not disturb the y dependence, it is sufficient to calculate only one-dimensional convolution over x coordinate for the sample-to-detector distance. It was calculated by means of double Fourier transformation using the Fourier image of the propagator which is known analytically. The fast Fourier transform (FFT) procedure was applied. Details can be found in Ref. 12. The com-

puter program is written in Java (Ref. 13) and ACL (advanced command language).[14]

We have found that the simulated images of the pipe with a 4 μm diameter match the experimental data better than the other pipes with different diameters. They are shown in the right-top panel of Fig. 2. These findings enabled us to define three essential parameters which characterize the two-dimensional (x,z) picture. The first parameter is the distance of focusing because the micropipe can play a role of a small x-ray lens.[15] The second one is the image contrast $(I_{\max}-I_{\min})/(I_{\max}+I_{\min})$. The third one is the increasing speed of a central white area between the black areas, as a function of the sample-to-detector distance. At first glance, this size looks like an effective pipe diameter. The bottom panels of Fig. 2 show the calculated images of the smaller and larger diameters of 3 and 5 μm. These simulated images enable us to estimate the accuracy of the pipe diameter and analyze the effects of the parameters discussed above on the diameter. The focus distance and the contrast are rather sensitive parameters which increase with the diameter. The speed parameter is higher for the smaller pipe. This behavior is similar to the Fraunhofer diffraction, although the criterion for this diffraction is not fulfilled.

In conclusion, we would like to note that the method of computer simulation is very promising for understanding the properties of the white beam phase contrast images of micropipes in SiC. In this work, we investigated only the distance dependence of the images, demonstrating that this dependence makes it possible to obtain enough information for a better comparison with the simulation. The micropipe in this study was aligned perpendicular to the beam. However, phase contrast image may significantly change with the orientation of micropipe. Furthermore, micropipes may not necessarily have round cross section. These questions call for further investigations.

The work of V.G.K. is supported by RFBR under Grant Nos. 05-02-16702, 07-02-00067a, and RS-6869.2006.2. The experimental part of this work is supported by the Creative Research Initiatives (Functional X-ray Imaging) of MOST/KOSEF and RFBR under Grant No. 06-02-16244.

[1] A. Snigirev, I. Snigireva, V. Kohn, S. Kuznetsov, and I. Schelokov, Rev. Sci. Instrum. **66**, 5486 (1995).
[2] M. Yu. Gutkin, A. G. Sheinerman, T. S. Argunova, J.-M. Yi, J.-H. Je, S. S. Nagalyuk, E. N. Mokhov, G. Margaritondo, and Y. Hwu, J. Appl. Phys. **100**, 093518 (2006).
[3] P. Cloetens, R. Barrett, J. Baruchel, J.-P. Guigay, and M. Schlenker, J. Phys. D **29**, 133 (1996).
[4] Y. Hwu, H. H. Hsieh, M. J. Lu, W. L. Tsai, H. M. Lin, W. C. Goh, B. Lai, J. H. Je, C. K. Kim, D. Y. Noh, H. S. Youn, G. Tromba, and G. Margaritondo, J. Appl. Phys. **86**, 4613 (1999).
[5] P. Krishna, S.-S. Jiang, and A. R. Lang, J. Cryst. Growth **71**, 41 (1985).
[6] X. R. Huang, M. Dudley, W. M. Vetter, W. Huang, S. Wang, and C. H. Carter, Appl. Phys. Lett. **74**, 353 (1999).
[7] F. C. Frank, Acta Crystallogr. **4**, 497 (1951).
[8] I. Kamata, H. Tsuchida, T. Jikimoto, and K. Izumi, Jpn. J. Appl. Phys., Part 1 **39**, 6496 (2000).
[9] M. Yu. Gutkin, A. G. Sheinerman, T. S. Argunova, E. N. Mokhov, J.-H. Je, Y. Hwu, W.-L. Tsai, and G. Margaritondo, Appl. Phys. Lett. **83**, 2157 (2003).
[10] Yu. A. Vodakov, A. D. Roenkov, M. G. Ramm, E. N. Mokhov, and Yu. A. Makarov, Phys. Status Solidi B **202**, 177 (1997).
[11] See http://henke.lbl.gov/opticalconstants/bend2.html for the SR spectrum.
[12] V. G. Kohn, I. I. Snigireva, and A. A. Snigirev, Crystallogr. Rep. **51**, S4 (2006).
[13] See http://java.sun.com for the programming language Java.
[14] See http://vkacl.narod.ru for the programming language ACL.
[15] A. Snigirev, V. Kohn, I. Snigireva, and B. Lengeler, Nature (London) **384**, 49 (1996).